Applied Mathematical and Computational Sciences
Volume 8, Issue 2, November 2016, Pages 43-66

CONSERVATIVE SCHEMES FOR THREE COUPLED NONLINEAR SCHRÖDINGER EQUATION

S. ERTUG and A. AYDIN

Mathematics Department
Atılım University
06836 Incek, Ankara, Turkey
E-mail: ayhan.aydin@atilim.edu.tr

Abstract

A nonlinear implicit energy conserving scheme and a linearly implicit mass conserving scheme are constructed for the numerical solution of a three-coupled nonlinear Schrödinger equation. Both methods are second order. The numerical experiments verify the theoretical results that while the nonlinear implicit scheme preserves the energy, the linearly implicit method preserves the mass of the system. In addition, the schemes are quite accurate in preservation of the other conserved quantities of the system. Elastic collision, creation of new vector soliton and fusion of soliton are observed in the solitary wave evolution. The numerical methods are proven to be highly efficient and stable in simulation of the periodic and solitary waves of the equation in long terms.

1. Introduction

We consider the 3-coupled nonlinear Schrödinger equation ([1])

$$i\frac{\partial \psi_1}{\partial t}+\alpha_1\frac{\partial^2 \psi_1}{\partial x^2}+(\sigma|\psi_1|^2+e|\psi_2|^2+\sigma|\psi_3|^2)\psi_1=0,$$

$$i\frac{\partial \psi_2}{\partial t}+\alpha_2\frac{\partial^2 \psi_2}{\partial x^2}+(e|\psi_1|^2+\sigma|\psi_2|^2+e|\psi_3|^2)\psi_2=0,$$

$$i\frac{\partial \psi_3}{\partial t}+\alpha_3\frac{\partial^2 \psi_3}{\partial x^2}+(\sigma|\psi_1|^2+e|\psi_2|^2+\sigma|\psi_3|^2)\psi_3=0, \qquad (1)$$

2010 Mathematics Subject Classification: 65M06, 35L65, 37M05, 74H15.
Keywords: three coupled nonlinear Schrödinger equation, conservative scheme, periodic wave, soliton.
Received July 1, 2016; Accepted November 28, 2016

in the region

$$\mathcal{D} = \{(x, t) : x_L \le x \le x_R, 0 \le t \le T\} \tag{2}$$

with the initial conditions

$$\psi_k(x, 0) = \psi_{k0}(x), \quad k = 1, 2, 3. \tag{3}$$

and the periodic boundary conditions

$$\psi_k(x_L, t) = \psi_k(x_R, t), \quad k = 1, 2, 3, \tag{4}$$

where $i = \sqrt{-1}$, $\psi_1(x, t)$, $\psi_2(x, t)$ and $\psi_3(x, t)$ represent slowly varying amplitude of the pulse envelope for the underlying physical system. It is common to normalize $\psi_k(x, t)$, $k = 1, 2, 3$ such that $| \psi_k(x, t) |^2$ represents the optical power. The independent variables t and x represents time and space variables respectively. The parameters α_k, $k = 1, 2, 3$ are the dispersion coefficients, σ is the Landau constants which describe the self modulation of the wave packets, and e is the wave-wave interaction coefficients which describe the cross-modulations of the wave packets. They are all real parameters and their values vary for different polarizations in nonlinear optics or for different kinds of basic flows in geophysical fluid dynamics. The system of equation (1) is a nonlinear dissipative partial differential equation with the third-order nonlinear effects in optical fibers. This equation arises as the governing model equation in several branches of physics including, for example, optics, fluid dynamics, quantum mechanics and biophysics (cf. [1, 2, 3, 4, 5, 6] and references therein). In reality, many nonlinear partial differential equations (PDEs) do not have exact solutions; even cannot be reduced to linear equations and their solutions mostly depend on numerical simulation. However, numerical methods may destroy the conserved quantities of the PDE. Therefore it is natural to construct some numerical methods that preserve the invariants of the PDE.

The solution of (1) has some conservation properties, namely the mass conservations

$$Q_1(t) = \int_{x_L}^{x_R} | \psi_1 |^2 dx = Q_1(0),$$

$$Q_2(t) = \int_{x_L}^{x_R} |\psi_2|^2 dx = Q_2(0),$$

$$Q_3(t) = \int_{x_L}^{x_R} |\psi_3|^2 dx = Q_3(0), \tag{5}$$

and the energy conservation

$$\mathcal{H}(t) = \frac{1}{2}\int_{x_L}^{x_R}\Big\{-\alpha_1\Big|\frac{\partial\psi_1}{\partial x}\Big|^2 - \alpha_2\Big|\frac{\partial\psi_2}{\partial x}\Big|^2 - \alpha_3\Big|\frac{\partial\psi_3}{\partial x}\Big|^2$$
$$e|\psi_1|^2|\psi_2|^2 + \sigma|\psi_1|^2|\psi_3|^2 + e|\psi_2|^2|\psi_3|^2$$
$$\frac{\sigma}{2}(|\psi_1|^4 + |\psi_2|^4 + |\psi_3|^4)\Big\}dx = \mathcal{H}(0). \tag{6}$$

These conservation laws would lead us to believe that solutions ought to exist globally and be stable [7]. Although the 3-CNLS system (1) is not integrable in the sense of inverse scattering method, there is a special case for which it is integrable, i.e. soliton solutions can be constructed. The 3-CNLS system (1) is integrable if $\alpha_1\alpha_2 = \alpha_2\alpha_3 = \alpha_1\alpha_3$, $(\alpha_3 - \alpha_1)\alpha_2\sigma = \alpha_1\alpha_3 e$, $(\alpha_3 - \alpha_1)\alpha_2 e = \alpha_1\alpha_3\sigma$, otherwise it is not integrable [8]. For non-integrable cases, where the parameters are different, numerical methods have to be used in order to understand different nonlinear phenomena that arise by the interaction of stable and unstable wave packets in the 3-CNLS system.

The system of equation (1) reduced to 2-CNLS equation when we omit one of the complex valued function $\psi_j(x, t)$, $j = 1, 2, 3$. There are many computational work for 2-CNLS equation. Some of the them are symplectic and multisymplectic schemes ([1, 18, 19]), the variational iteration method [20], the Hopscothch method [21], Galerkin finite element method [22], and a fourth-order explicit Runge-Kutta method [23]. Recently, the main attention for the 2-CNLS equation is finite difference conservative schemes [24, 25, 26, 27]. However, they are not completely systematic either in their derivation or in their applicability. Although there are numerous works for the 2-CNLS equation, theoretical and numerical works for the 3-CNLS equation (1) are limited. In [9], exact bright one-soliton and two-soliton solutions for $\alpha_j = 1$, $(j = 1, 2, 3)$ and $\sigma = e$ have been obtained and some shape changing collisions have been given. Some new solutions have been reported in [10].

Explicit partially coherent soliton solutions have been obtained in [11, 12]. Exact dark soliton solutions have been given in [13]. A new periodic wave solution is obtained and its stability analysis is discussed in [1]. Several computational methods have been proposed for the system of equation (1) such as six-point multisymplectic scheme [1], semi-explicit multi-symplectic splitting scheme [14]. In [17], various split-step spectral (SSSP) scheme are proposed. They are proved to be mass conserving and to admit the exact plane wave solution. In [15] a new central difference and quartic spline approximation based exponential time differencing Crank-Nicolson (ETD-CN) method are used for the numerical solution of 3-CNLS equation (1). In [16] a new version of Cox and Matthews third order exponential time differencing Runge-Kutta (ETD3RK) scheme based on the (1, 2)-Padé approximation to the exponential function is introduced and some numerical results are presented for the discrete solution of the equation (1). But none of these methods are energy preserving. Up to the authors' knowledge there are no numerical studies on the energy preservation of the 3-CNLS equation in the literature. Therefore, it is still very challenging to develop an energy preserving scheme for the 3-CNLS equation. In this paper, an implicit energy conserving numerical scheme and a linearly implicit mass conserving scheme are proposed for the numerical solution of the 3-CNLS equation. The energy conserving scheme is developed based on the Average Vector Field (AVF) method. The AVF method is first introduced in [28]. In [29] it is described as a novel class of *B*-series methods that preserves energy for all (canonical) Hamiltonian vector fields. An extension of the AVF method to the canonical and non-canonical Hamiltonian systems are discussed in [30, 31]. In [32] AVF method is applied to Hamiltonian partial differential equations (PDEs) with constant symplectic structure. In [33] AVF method is applied to some PDEs in bi–Hamiltonian form with nonconstant Poisson structure. The energy preserving AVF method is applied to the coupled Schrödinger-KdV equations in [34]. In [35] a high order energy preserving scheme for the strongly coupled nonlinear Schrödinger system is proposed by using the AVF method. In addition to approximation of PDEs, the approximation of functions by trigonometric or algebraic polynomials is also an important topic of mathematical studies. Function approximation has many application areas such as data representation, signal processing, numerical analysis, and solutions of differential equations (see, for example [36, 37, 38, 39, 40]).

This paper is organized as follows. In section 2, a fully implicit energy conserving scheme and a linearly implicit mass conserving scheme are proposed to the 3-CNLS equation (1). In section 3 some numerical experiments are carried out to show the efficiency and reliability of the proposed schemes in long term integration. The paper ends with a brief conclusion in section 4.

2. Numerical Schemes

To establish the numerical approximation schemes for the 3-CNLS equation (1), the rectangular domain $\mathcal{D}$ in (2) is divided into small grids by the parallel lines $x = x_j (j = 1, 2, \ldots, M+1)$ and $t = t_n (n = 0, 1, \ldots, N)$, where $x_j = x_L + jh$, $t_n = n\tau$, and $Mh = x_R - x_L$, $N\tau = T (j = 1, 2, \ldots, M+1; n = 0, 1, \ldots, N)$. Here $h = \Delta x$ and $\tau = \Delta t$ are spatial and temporal step sizes, respectively. Let $\mathbf{z}_{j,n}$ be the approximation to the exact solution $\mathbf{z}(x_j, t_n)$ at the regular grid point (x_j, t_n). The periodic boundary condition is used in all numerical methods. We propose the following two conservative schemes for the numerical integration of the 3-CNLS equation (1).

2.1. An implicit energy conserving scheme

We decompose the complex valued functions ψ_1, ψ_2 and ψ_3 into real and imaginary parts by using

$$\psi_1(x, t) = a(x, t) + ib(x, t),\ \psi_2(x, t) = u(x, t) + iv(x, t),$$
$$\psi_3(x, t) = p(x, t) + iq(x, t) \tag{7}$$

and defining $\mathbf{z} = (a, p, u, b, q, v)^T \in \mathbb{R}^6$, the 3-CNLS equation (1) can be expressed as the infinite dimensional Hamiltonian form

$$\mathbf{z}_t = \mathcal{J}\left(\frac{\delta \mathcal{H}}{\delta \mathbf{z}}\right) \tag{8}$$

with the skew-symmetric matrix defined by

$$\mathcal{J} = \begin{pmatrix} 0 & -\mathbf{I} \\ \mathbf{I} & 0 \end{pmatrix},$$

where **0** and **I** are the zero and identity matrices of dimension 3. Here the variational derivative is given by

$$\frac{\delta \mathcal{H}}{\delta \mathbf{z}} = \int H(\mathbf{z},\ \mathbf{z}_x)dx = \frac{\partial H}{\partial \mathbf{z}} - \partial_x\left(\frac{\partial H}{\partial \mathbf{z}_x}\right) + \partial_{xx}\left(\frac{\partial H}{\partial \mathbf{z}_{xx}}\right) - \ldots.$$

For the system (1), the Hamiltonian $\mathcal{H}$ is the energy defined by (6). For the numerical treatment, the second order spatial differential operator $\frac{\partial^2}{\partial x^2}$ is discretized as

$$\frac{\partial^2 \psi}{\partial x^2} \approx \frac{\psi_{j-1} - 2\psi_j + \psi_{j+1}}{\Delta x^2}$$

so that the infinite Hamiltonian system (8) is reduced to the finite-dimensional Hamiltonian system

$$\frac{d\mathbf{Z}}{dt} = \mathbf{J}\nabla H(\mathbf{Z}) \tag{9}$$

corresponding to the system (1). Here $\mathbf{Z} = (\mathbf{a}, \mathbf{b}, \mathbf{p}, \mathbf{q}, \mathbf{u}, \mathbf{v})^T$, $\mathbf{a} = (a_1, a_2, \ldots, a_M)$, $\ldots$, $\mathbf{v} = (v_1, v_2, \ldots, v_M)$,

$$\begin{aligned} H(\mathbf{Z}) = \frac{\Delta x}{2}\sum_{j=1}^{M}\Bigg\{ & -\alpha_1\left(\frac{a_{j+1} - a_j}{\Delta x}\right)^2 - \alpha_1\left(\frac{b_{j+1} - b_j}{\Delta x}\right)^2 \\ & - \alpha_2\left(\frac{p_{j+1} - p_j}{\Delta x}\right)^2 - \alpha_2\left(\frac{q_{j+1} - q_j}{\Delta x}\right)^2, \\ & - \alpha_3\left(\frac{u_{j+1} - u_j}{\Delta x}\right)^2 - \alpha_3\left(\frac{v_{j+1} - v_j}{\Delta x}\right)^2, \\ & + e(a_j^2 + b_j^2)(p_j^2 + q_j^2) + \sigma(a_j^2 + b_j^2)(u_j^2 + v_j^2) \\ & + e(p_j^2 + q_j^2)(u_j^2 + v_j^2) \Bigg\} \end{aligned} \tag{10}$$

is the discrete analog of the energy $\mathcal{H}(\mathbf{z})$ in (6) and

$$\mathbf{J} = \begin{pmatrix} \overline{\mathbf{0}} & -\overline{\mathbf{I}} \\ \overline{\mathbf{I}} & \overline{\mathbf{0}} \end{pmatrix}, \tag{11}$$

where $\bar{\mathbf{0}}$ and $\bar{\mathbf{I}}$ are zero and identity matrices of dimension $3M$. Then, we discretize the system of the ordinary differential equations (9) in time by using the second order AVF method [28, 32] and obtain

$$\frac{\mathbf{Z}_{n+1} - \mathbf{Z}_n}{\Delta t} = \mathbf{J} \int_0^1 \nabla H((1-\xi)\mathbf{Z}_n + \xi \mathbf{Z}_{n+1}) d\xi. \tag{12}$$

The scheme (12) is a discrete gradient scheme and preserves the energy (10) without any restriction of at every time step [28]. In order to show this, we take the scalar product of both sides of the system (12) by

$$\left(\int_0^1 \nabla H((1-\xi)\mathbf{Z}_n + \xi \mathbf{Z}_{n+1}) d\xi \right)^T. \tag{13}$$

Then, the right-hand side of (12) becomes zero by the skew-symmetry of the matrix $\mathbf{J}$. It follows that the left-hand side of (12) reduced to

$$\int_0^1 (\mathbf{Z}_{n+1} - \mathbf{Z}_n) \cdot \nabla H((1-\xi)\mathbf{Z}_n + \xi \mathbf{Z}_{n+1}) d\xi = 0, \tag{14}$$

i.e.

$$\int_0^1 \frac{d}{d\xi} H((1-\xi)\mathbf{Z}_n + \xi \mathbf{Z}_{n+1}) d\xi = 0, \tag{15}$$

and

$$H(\mathbf{Z}_{n+1}) = H(\mathbf{Z}_n). \tag{16}$$

So that we get

$$H(\mathbf{Z}_n) = H(\mathbf{Z}_{n-1}) = \ldots = H(\mathbf{Z}_0). \tag{17}$$

The existence of the above discrete energy conservation law (16) guarantee that the numerical scheme will not blow-up and the scheme (12) will be stable [41, 42]. The local truncation error of the scheme (12) is complicated and will not be explored here. For linear vector field, the scheme is reduced to the implicit midpoint rule. In conservative schemes, the temporal order of a scheme may need to be much greater than the spatial order. The temporal order plays an important role in long-time integration. The method (12) is second order convergence in time. Generalization of the method (12) to higher

order can be obtained in [29]. For polynomial Hamiltonian (10), the integral in (12) is evaluated exactly. The scheme (12) will be compared with the linearly implicit scheme presented in the following section.

2.2. A linearly implicit mass conserving scheme

Following [27, 41], we propose the linearly implicit two–level scheme (LIS) for the numerical solution of (1)

$$i\frac{\psi_{1,j}^{n+1}-\psi_{1,j}^{n-1}}{2\Delta t}+\frac{\alpha_1}{2}\left(\frac{\psi_{1,j-1}^{n+1}-2\psi_{1,j}^{n+1}+\psi_{1,j+1}^{n+1}}{\Delta x^2}+\frac{\psi_{1,j-1}^{n-1}-2\psi_{1,j}^{n-1}+\psi_{1,j+1}^{n-1}}{\Delta x^2}\right)$$

$$+(S_1)_j^n\left(\frac{\psi_{1,j}^{n+1}+\psi_{1,j}^{n-1}}{2}\right)=0$$

$$i\frac{\psi_{2,j}^{n+1}-\psi_{3,j}^{n-1}}{2\Delta t}+\frac{\alpha_2}{2}\left(\frac{\psi_{2,j-1}^{n+1}-2\psi_{2,j}^{n+1}+\psi_{2,j+1}^{n+1}}{\Delta x^2}+\frac{\psi_{2,j-1}^{n-1}-2\psi_{2,j}^{n-1}+\psi_{2,j+1}^{n-1}}{\Delta x^2}\right)$$

$$+(S_2)_j^n\left(\frac{\psi_{2,j}^{n+1}+\psi_{2,j}^{n-1}}{2}\right)=0$$

$$i\frac{\psi_{3,j}^{n+1}-\psi_{3,j}^{n-1}}{2\Delta t}+\frac{\alpha_3}{2}\left(\frac{\psi_{3,j-1}^{n+1}-2\psi_{3,j}^{n+1}+\psi_{3,j+1}^{n+1}}{\Delta x^2}+\frac{\psi_{3,j-1}^{n-1}-2\psi_{3,j}^{n-1}+\psi_{3,j+1}^{n-1}}{\Delta x^2}\right)$$

$$+(S_1)_j^n\left(\frac{\psi_{3,j}^{n+1}+\psi_{3,j}^{n-1}}{2}\right)=0 \qquad (18)$$

where

$$(S_1)_j^n=\sigma|\psi_{1,j}^n|^2+e|\psi_{2,j}^n|^2+\sigma|\psi_{3,j}^n|^2,(S_2)_j^n=e|\psi_{1,j}^n|^2+\sigma|\psi_{2,j}^n|^2+e|\psi_{3,j}^n|^2.$$

This method is a linearly implicit method and a not self-starting method. In order to start the iteration in (18), two initial values ψ_j^0 and ψ_j^1 are required. ψ^0 is obtained from the initial condition. ψ^1 will be obtained from the Forward Euler method with a small step size $\Delta t = 0.0001$. Then, ψ^2, ψ^3, … are obtained from the two-step scheme (18).

Theorem 2.2.1. *The two-level scheme* (18) *is conservative in the sense*

$$Q_1^n = \sum_{j=1}^{M}(|\psi_{1j}^{n+1}|^2 + |\psi_{1j}^{n}|^2) = Q_1^{n-1} = \ldots = Q_1^0$$

$$Q_2^n = \sum_{j=1}^{M}(|\psi_{2j}^{n+1}|^2 + |\psi_{2j}^{n}|^2) = Q_2^{n-1} = \ldots = Q_2^0$$

$$Q_3^n = \sum_{j=1}^{M}(|\psi_{3j}^{n+1}|^2 + |\psi_{3j}^{n}|^2) = Q_3^{n-1} = \ldots = Q_3^0 \tag{19}$$

for $n = 0, 1, 2, \ldots, N$ *where* Q_1^n, Q_2^n, *and* Q_3^n *are discrete masses.*

Proof. In order to show that the proposed scheme (18) has conserved quantity Q_1^n, we multiply the first equation in (18) by $(\overline{\psi_{1,j}^{n+1}} + \overline{\psi_{1,j}^{n-1}})$ and take the sum over m. The first term in the multiplication gives

$$i(\overline{\psi_{1,j}^{n+1}} + \overline{\psi_{1,j}^{n-1}})\frac{\psi_{1,j}^{n+1} - \psi_{1,j}^{n-1}}{2\Delta t} = \frac{i}{2\Delta t}(|\psi_{1,j}^{n+1}|^2 - |\psi_{1,j}^{n-1}|^2) + \text{Real terms.} \tag{20}$$

The second term $\frac{\alpha_1}{2}(\overline{\psi_{1,j}^{n+1}} + \overline{\psi_{1,j}^{n-1}})\left(\frac{\psi_{1,j-1}^{n+1} - 2\psi_{1,j}^{n+1} + \psi_{1,j+1}^{n+1}}{\Delta x^2} + \frac{\psi_{1,j-1}^{n-1} - 2\psi_{1,j}^{n-1} + \psi_{1,j+1}^{n-1}}{\Delta x^2}\right)$ and the third term $(S_1)_j^n(\overline{\psi_{1,j}^{n+1}} + \overline{\psi_{1,j}^{n-1}})\left(\frac{\psi_{1,j}^{n+1} + \psi_{1,j}^{n-1}}{2}\right)$ in the multiplication give real values under periodic boundary conditions. Taking the imaginary terms in this multiplication, we get

$$\sum_{j=1}^{M}|\psi_{1,j}^{n+1}|^2 - |\psi_{1,j}^{n-1}|^2 = 0$$

which gives

$$\sum_{j=1}^{M}|\psi_{1,j}^{n+1}|^2 + |\psi_{1,j}^{n}|^2 = \sum_{j=1}^{M}|\psi_{1,j}^{n}|^2 + |\psi_{1,j}^{n-1}|^2$$

$$Q_1^n = Q_1^{n-1}.$$

This completes the proof of the first conserved quantity $Q_1^n = Q_1^0$. Other conserved quantities $Q_2^n = Q_2^0$ and $Q_3^n = Q_3^0$ can be shown similarly.

2.2.1. Accuracy, stability and convergence of the scheme

Using the Taylor series expansions about (x_m, t_n) of all terms in the scheme (18), we get the principal part of the local truncation error

$$\frac{(\Delta t)^2}{6}\psi_{k,ttt} + \frac{(\Delta x)^2}{12}\psi_{k,xxxx} + \frac{(\Delta t)^2}{2}\psi_{k,xxtt} + \frac{(\Delta t)^2}{2}S1_m^n\psi_{k,tt}, \tag{21}$$

where $k = 1, 2, 3$. This shows that the proposed scheme (18) is of order $\mathcal{O}((\Delta t)^2) + \mathcal{O}((\Delta x)^2)$. The proposed scheme is consistent since the principal part of the local truncation error goes to zero as $\Delta x, \Delta t \to 0$.

To study stability of this scheme, let $\psi_{k,j}^n \approx Z_j^n$, and consider the linearized form

$$\frac{Z_j^{n+1} - Z_j^{n-1}}{2\Delta t} + \frac{\alpha_k}{2}\left(\frac{Z_{j-1}^{n+1} - 2Z_j^{n+1} + Z_{j+1}^{n+1}}{\Delta x^2} + \frac{Z_{j-1}^{n-1} - 2Z_j^{n-1} + Z_{j+1}^{n-1}}{\Delta x^2}\right)$$

$$+ \widetilde{S}\left(\frac{Z_j^{n+1} + Z_j^{n-1}}{2}\right) = 0, \tag{22}$$

where the constant term $\widetilde{S} = \max_{j=1,\ldots,M}\{S_{1j}^n, S_{2j}^n\}$. By von Neumann stability analysis, we substitute

$$Z_j^n = \xi^n e^{i\beta j\Delta x}, \quad i^2 = -1 \tag{23}$$

into (22), and get

$$|\xi|^2 = \frac{i - \left(\widetilde{S}\Delta t - 4r\sin^2\left(\frac{\beta\Delta x}{2}\right)\right)}{i + \left(\widetilde{S}\Delta t - 4r\sin^2\left(\frac{\beta\Delta x}{2}\right)\right)}$$

and

$$|\xi| = 1,$$

where $r = \dfrac{\Delta t}{\Delta x^2}$. This shows the two-step scheme (18) is unconditionally stable in the linear sense. For the convergency of the scheme we will refer to the Lax equivalence theorem which is only applied to well-posed linear initial-value problems. Although the 3-CNLS equation (1) is a nonlinear PDE, experience show that stability criteria for the linearized finite difference scheme can be effective in practice. The nonlinear finite difference scheme that is consistent and whose linearized equivalent is stable generally converge, even for nonlinear finite difference scheme [43, 44].

3. Numerical Results

In this section, several test problems are applied to show the efficiency and accuracy of the proposed numerical scheme (18). In all computations we choose $\alpha_1 = \alpha_2 = \alpha_3 = 1$ and $\sigma = 1$. Conservation of the mass and the energy are measured by looking the error norms

$$\| E \|_\infty = \max_{1\le n\le N} \left| \frac{E^n - E^0}{E^n} \right|, \| Q_k \|_\infty = \max_{1\le n\le N} \left| \frac{Q_k^n - Q_k^0}{Q_k^0} \right|, \tag{24}$$

where $k = 1, 2, 3$ and E^0, Q^0 are the initial discrete energy and mass, and E^n, Q^n are discrete energy and mass at $t = n\Delta t$, respectively. Here E^n is the hamiltonian (10). The discrete masses Q_k^n are defined as $\sum_{j=1}^{M} |\psi_{kj}^n|^2$ for the AVF scheme. The discrete masses (19) are used for the LIS.

3.1. Unstable periodic wave solution

In the first test we will look at the evolution of unstable periodic wave of the 3-CNLS equation (1) with $e = 1$. The following initial conditions are used [1]

$$\psi_1(x) = 0.2[1 - 0.1\cos(\ell x)],\ \psi_2(x) = 0.3[1 - 0.1\cos(\ell(x + \theta))],$$
$$\psi_3(x) = 0.2[1 - 0.1\cos(\ell x)], \tag{25}$$

where θ is the phase difference. We choose $\ell = 0.5$ which implies that the plane wave (25) is unstable. We solved the problem (1)-(4) on the interval $-4\pi \le x \le 4\pi$ with $M = 128$ spatial grid points and a time step of length

$\Delta t = 5 \times 10^{-3}$ and compare the schemes (12) and (18) with the Exponential time differencing Crank-Nicolson (ETD-CN) method with a quartic spline interpolation approximation [15] and the multisymplectic six-point scheme [1]. For comparative purpose we compute $\| \psi_1 \|_2^2$ and $\| \psi_2 \|_2^2$ and used the same error $| \| \psi(\cdot, T) \|_2^2 - \| \psi(\cdot, 0) \|_2^2 |$ as in [15]. Since the value of $\| \psi_3 \|_2^2$ is same with $\| \psi_1 \|_2^2$, it is not presented in the test. According to the initial values (25), the exact values of $\| \psi_1 \|_2^2$ and $\| \psi_2 \|_2^2$ at $t = 0$ are 1.00515481265051 and 1.50773221897576, respectively. From the Table 1 we see that the linearly implicit scheme (LIS) (18) conserves mass $\| \psi_j \|_2^2$, $j = 1, 2$ exactly. Moreover, the AVF scheme (12) preserves the mass better than the multisymplectic six-point scheme [1] and the Exponential time differencing Crank-Nicolson (ETD-CN) method with a quartic spline interpolation approximation [15]. Figure 1 represents the surface of the destabilized periodic waves ψ_1 and ψ_2 for $\theta = 0$ and $\theta = 7\pi/4$ up to $T = 80$, by using the AVF scheme (12). The two-step scheme (18) represents the same surfaces, which are not shown here. From the figure we see that both schemes well simulate the periodic wave. We also see that addition of a phase difference to the wave ψ_2 affects the evolution of wave and decrease the number of oscillations (see [1]).

Table 1. Comparison of conservations in $\| \psi_j \|_2^2$, $j = 1, 2$, via the multisymplectic six-point scheme [1], the Exponential time differencing Crank-Nicolson (ETD-CN) method with a quartic spline interpolation approximation [15] and the scheme (18)

	$\| \psi_1 \|_2^2$		$\| \psi_2 \|_2^2$	
	$T = 20$	$T = 80$	$T = 20$	$T = 80$
Error in [1]	$5.7e-04$	$3.2e-05$	$8.7e-04$	$8.0e-05$
Error in [15]	$1.1e-05$	$2.2e-05$	$5.4e-05$	$6.0e-05$
Error in AVF	$1.4e-07$	$9.4e-09$	$2.2e-07$	$1.4e-08$
Error in TSM	$2.5e-14$	$1.0e-13$	$3.8e-14$	$1.4e-13$

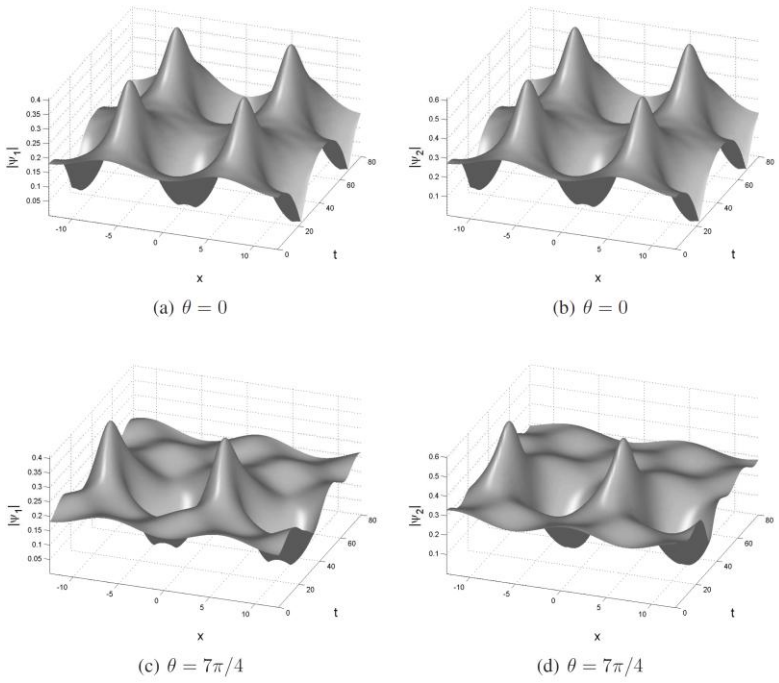

Figure 1. Surfaces of destabilized waves via the 2-step scheme (18). Effect of the phase difference θ.

3.2. Solitary wave solution

We consider the 3-CNLS equation (1) with the initial condition

$$\psi_1(x, 0) - \sqrt{2}r_1\text{sech}\,(r_1x + x_{10})\exp(iv_1x),$$

$$\psi_2(x, 0) - \sqrt{2}r_2\text{sech}\,(r_2x - x_{20})\exp(-iv_2x),$$

$$\psi_3(x, 0) - \sqrt{2}r_3\text{sech}\,(r_3x + x_{30})\exp(iv_3x), \tag{26}$$

to see the evolution of solitary wave solution. In the initial conditions (26), $\psi_1(x, 0)$ represents a solitary wave located initially at the position x_{10} with velocity v_1.

3.2.1. Elastic collision $(e = 1)$:

We consider the problem (1)-(4) in the region $-40 \le x \le 40$ so that the boundaries do no effect the solitary wave propagation. We take

$M = 400$, $\Delta t = 0.02$, $r_1 = r_2 = r_3 = 1.0$, $v_1 = v_2 = 1.0$, $v_3 = 1/4$, $x_{10} = x_{20} = 10$ and $x_{30} = 30$. Table 2 displays some errors correspond to the AVF scheme (12) and the LIS scheme (18) for various space and time steps. It can be seen from the Table 2 that both scheme produce remarkable reduction in the errors when the step sizes are reduced and convergence is evident. Figure 2 represents the evolution of solitary waves for $0 \le t \le 20$ and $e = 1$. From the figure we see that the waves ψ_1 and ψ_3 moves to the right, while the wave ψ_2 move to the left in time. At the time $t = 20$ collision phenomena occurs. During collision we observe a decrease in the amplitudes of the waves, but after the collision there is a roundup in the amplitudes. We see that the after collisions, the waves move forward in the same direction and three waves emerge without change in their shapes and velocities. This shows that the collision is elastic. In the context of biophysics the Figure 2 shows the interaction of three solitions during theirs propagation through the alpha helical protein chain [4]. From the Figure 2(d), we can conclude that the total energy of the three solitions are found to be conserved and there is no change in the distribution of energy among them in the neighbouring spines keeping the total energy conserved. Table 3 shows the errors in conservations properties (5) and (6). From the table we see that while the AVF scheme (12) preserves the energy (6) better than the linearly implicit scheme (18), the linearly implicit scheme (18) preserves the masses (5) better than the AVF scheme (12). In addition to the Table 3, the Figure 3 verifies the theoretical results (17) and the Theorem 2.2.1.

Table 2. Accuracy in solitary wave solution at time $T = 1$.

	Δx	Δt	$\| Q_1 \|_\infty$	$\| Q_2 \|_\infty$	$\| Q_3 \|_\infty$	$\| E \|_\infty$
	0.25	0.25	$1.0e-3$	$1.3e-3$	$4.6e-5$	$3.8e-10$
		0.125	$7.9e-5$	$7.9e-5$	$1.3e-5$	$1.2e-11$
AVF		0.0625	$6.1e-6$	$6.1e-6$	$1.3e-6$	$2.6e-11$
	0.125	0.125	$6.1e-5$	$6.1e-5$	$2.7e-6$	$2.3e-10$
		0.0625	$5.2e-6$	$5.2e-6$	$8.2e-7$	$4.9e-11$
	0.25	0.25	$1.1e-15$	$1.1e-15$	$1.9e-15$	$7.1e-1$
		0.125	$1.7e-15$	$8.8e-16$	$1.3e-15$	$3.8e-1$
LIS		0.0625	$4.4e-16$	$2.2e-16$	$4.4e-16$	$1.3e-1$
	0.125	0.125	$9.7e-15$	$5.1e-15$	$5.1e-15$	$3.2e-1$
		0.0625	$2.8e-15$	$1.5e-15$	$2.2e-15$	$1.7e-1$

Table 3. Errors at time $T = 20$ in solitary wave solution.

		$\| Q_1 \|_\infty$	$\| Q_2 \|_\infty$	$\| Q_3 \|_\infty$	$\| E \|_\infty$
	$T = 10$	$2.67e-5$	$2.67e-5$	$7.77e-7$	$2.97-10$
AVF	$T = 20$	$2.67e-5$	$2.67e-5$	$6.36e-5$	$5.44-10$
	$T = 10$	$1.97e-14$	$1.77e-14$	$1.99e-14$	$5.70-02$
LIS	$T = 20$	$3.46e-14$	$3.19e-14$	$3.64e-14$	$5.07-02$

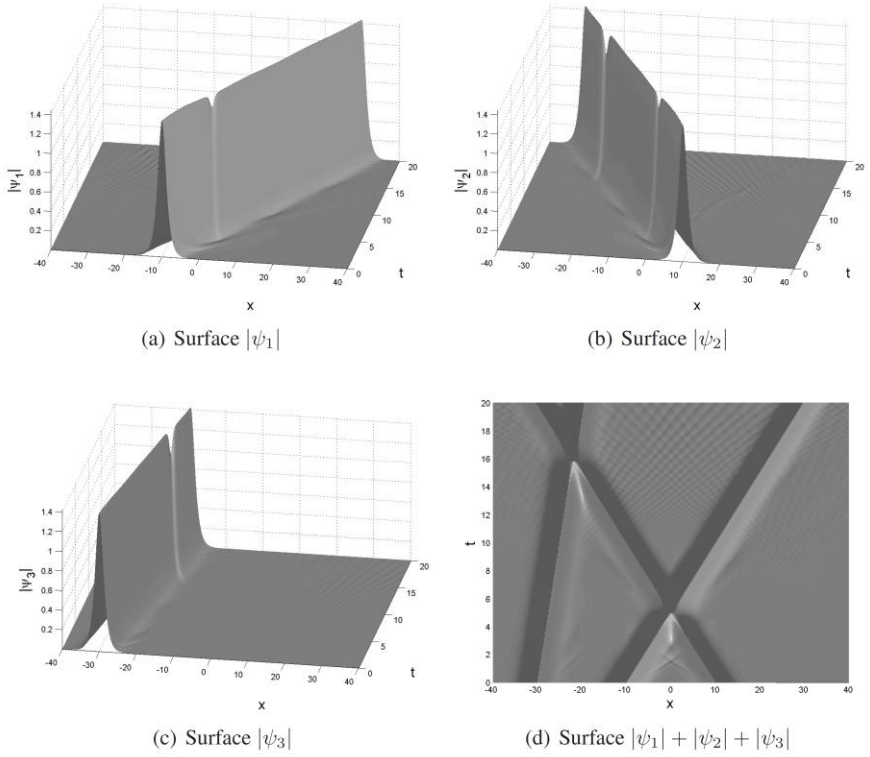

(a) Surface $|\psi_1|$ (b) Surface $|\psi_2|$

(c) Surface $|\psi_3|$ (d) Surface $|\psi_1| + |\psi_2| + |\psi_3|$

Figure 2. Solitary wave evolutions.

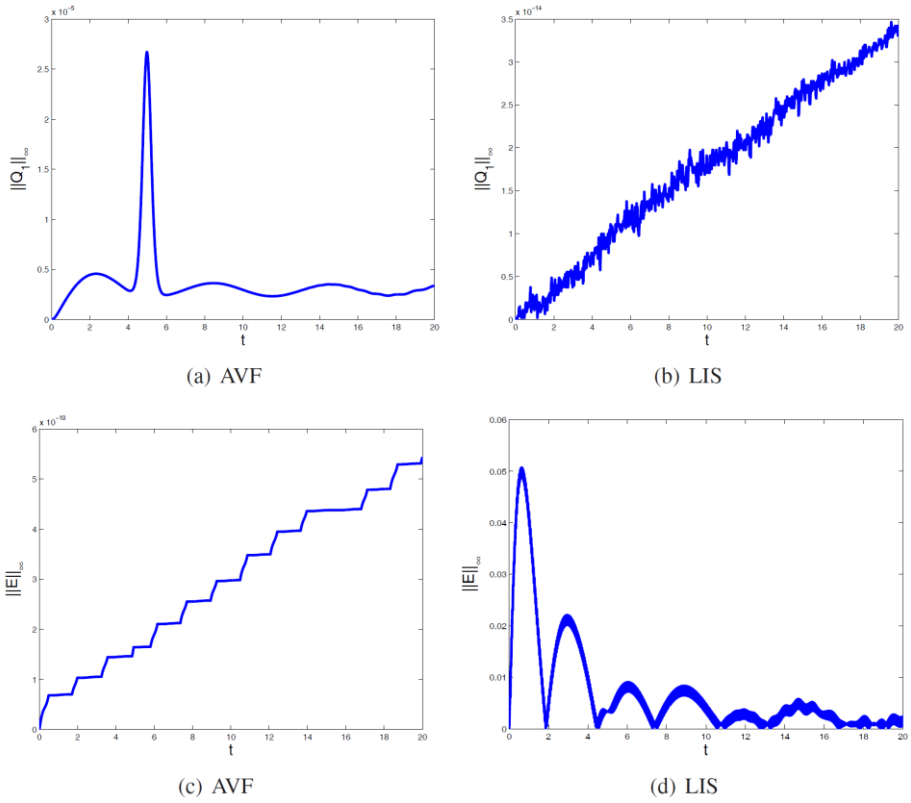

Figure 3. Errors in solitary wave evolutions.

3.2.2. Creation of new vector soliton $(e = 2)$ **and fusion** $(e = 0.35)$:

In this example, we present creation of new vector soliton and fusion scenarios of three solitary wave solutions. First we choose the wave-wave interaction coefficient $e = 2$. The following parameters are used in this test:

$$r_1 = 1.0, r_2 = 1.2, r_3 = 1.3, v_1 = 1/4, v_2 = 1/4, v_3 = 1/2, x_{10} = x_{20} = 10, x_{30} = 30.$$

Figure 4 is obtained by the linearly implicit scheme (18) over the spatial domain $-40 \le x \le 40$ up to $T = 29$ for the values $M = 400$ and $\Delta t = 0.01$. Same results are obtained by means of the AVF scheme (12) which is not shown here. From the figure, we see that the collisions takes place between the time interval $15 \le t \le 20$. We can see the creation of new vector soliton after the collision of three soliton. Figure 5 represents the error of mass

conservation and the energy conservation in the collision. From the figure, we can see that mass errors of the numerical solutions are very small. Therefore, we can say that creation of new vector solitons are not the consequence of numerical errors. We note that collision take place about the time $t \approx 15$. We can see that after the collision there is a violation in the preservation of the energy by the AVF scheme. The errors in mass conservation by the LIS are within the roundoff error of machine. If we chance the wave-wave interaction coefficient e and choose $e = 0.35$ we observe the fusion of three soliton in Figure 6. Figure 7 shows the errors in the fusion scenario. Figures 5 and 7 verify the energy conservation of the energy by the AVF scheme (12) and mass conservation of the scheme (18) as proven in Theorem 2.2.1.

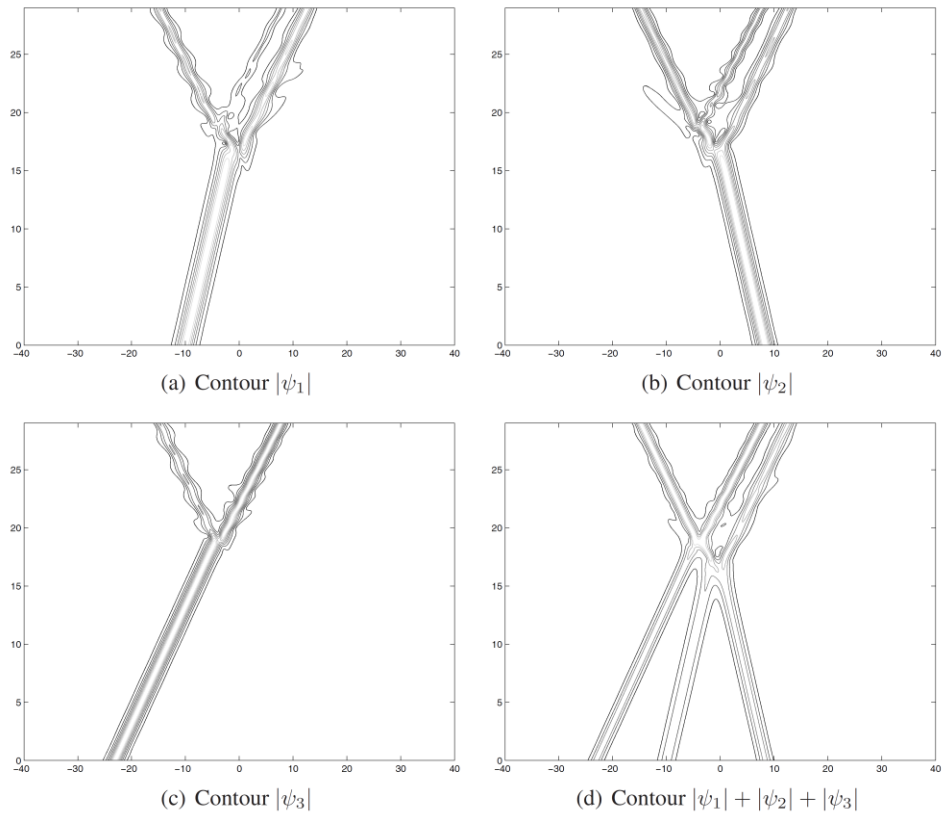

Figure 4. Creation of vector soliton with $e = 2$.

4. Conclusion

In the present paper, two new methods for the numerical solution of the coupled nonlinear Schrödinger (3-CNLS) equations are proposed and analyzed. The first method is nonlinear and energy conserving. It is proposed by using the average vector field method for the time discretization of the equation. The second method is linearly implicit and mass conserving. The preservation of energy and the mass are illustrated numerically. Wave-wave interaction scenarios are investigated and elastic collision, creation of new vector soliton and fusion of soliton are observed in numerical simulation. Numerical results confirm the excellent long time behavior of the proposed schemes by preserving energy and mass.

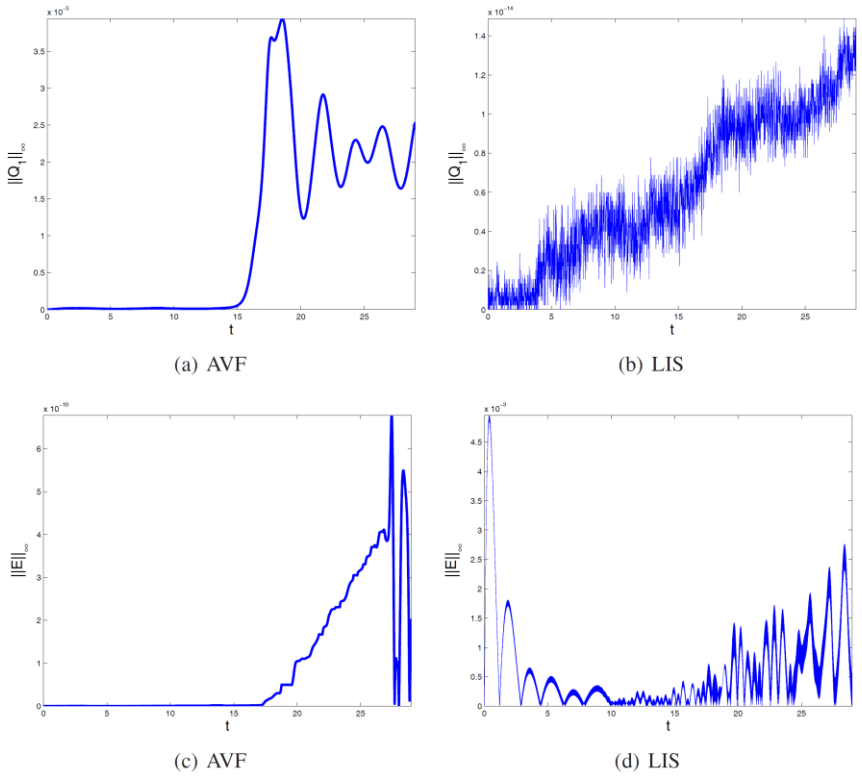

Figure 5. Errors in creation of vector soliton with $e = 2$.

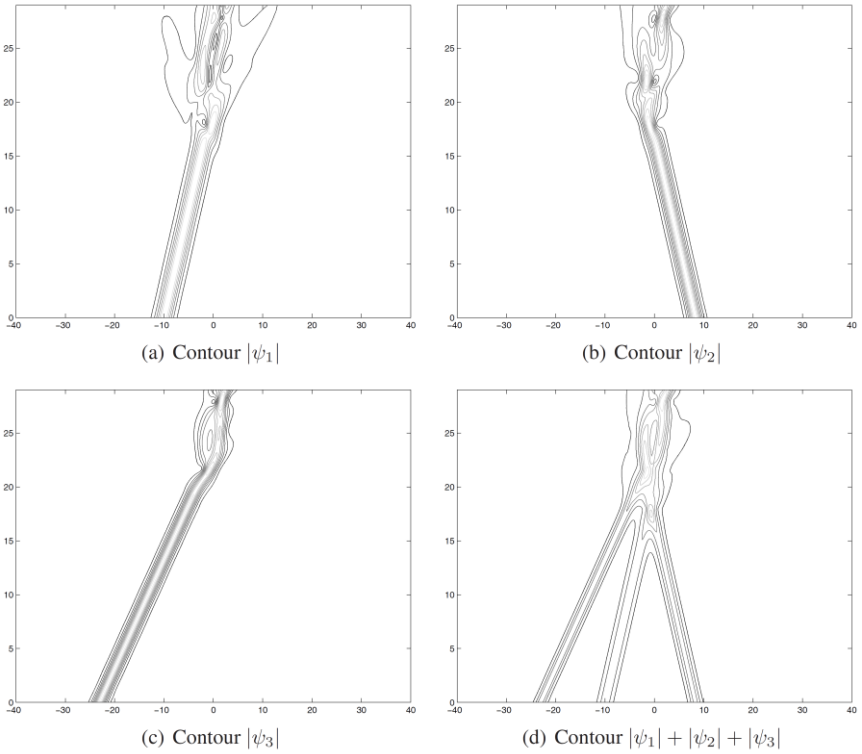

(a) Contour $|\psi_1|$ (b) Contour $|\psi_2|$

(c) Contour $|\psi_3|$ (d) Contour $|\psi_1| + |\psi_2| + |\psi_3|$

Figure 6. Fusion of three soliton with $e = 0.35$.

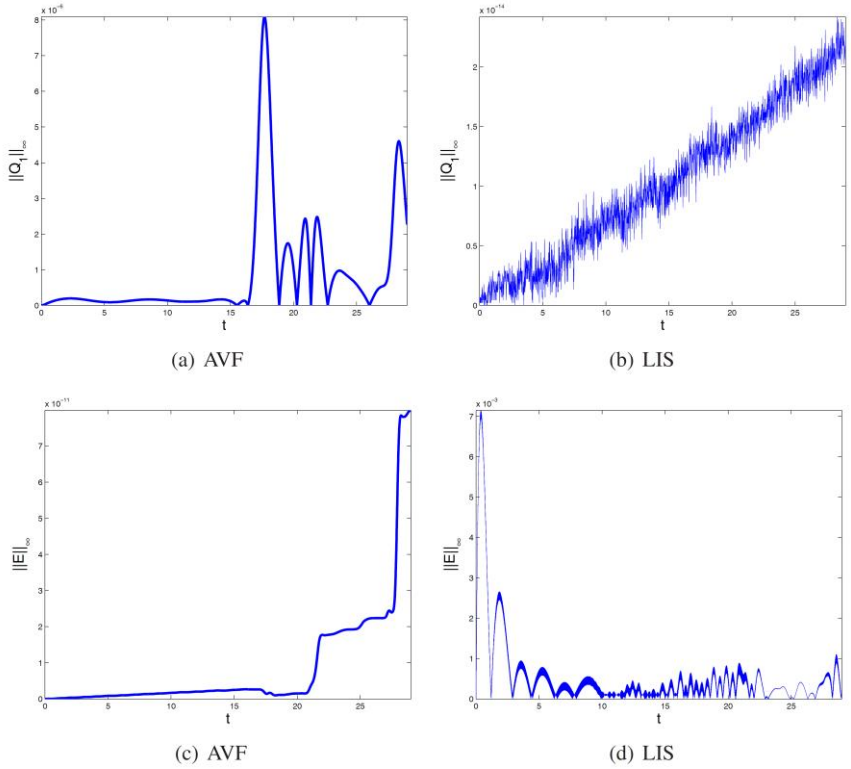

Figure 7. Errors in fusion of three soliton with $e = 0.35$.

Acknowledgements

This work is supported by The Scientific and Technological Research Council of Turkey (TUBITAK) with the project number 114F020.

References

[1] A. Aydin, Multisymplectic integration of *N*-coupled nonlinear Schrödinger equation with destabilized periodic wave solutions, Chaos, Solitons and Fractals 41 (2009), 735-751.

[2] G. P. Agrawal, Nonlinear Fiber Optics, Second Ed., Academic Press, New York, 1995.

[3] A. Akhmediev and A. Ankiewicz, Solitons: Nonlinear Pulses and Beams, Chapman and Hall, London, 1997.

[4] A. C. Scott, Physica Scripta 29 (1984), 279-283.

[5] Y. S. Kivshar and G. P. Agrawal, Optical Solitons: From Fibers to Photonic Crystals, Academic Press, San Diego, USA, 2003.

[6] C. C. Mei, The Applied Dynamics of Ocean Waves, World Scientific, Singapore, 1989.

[7] G. M. Penna and L. A. J. Medeiros, Contemporary Developments in Continuum Mechanics and Partial Differential Equations: Proceedings of the International Symposium on Continuum Mechanics and Partial Differential Equations, Rio de Janeiro, North-Holland, 1977.

[8] K. Porsezian, Bilinerization of Coupled Nonlinear Schrödinger Type Equations: Integrability and Solitons, J. Nonlinear Mathematical Physics 5(2) (1998), 26-131.

[9] T. Kanna and M. Lakshmanan, Exact Soliton Solutions, Shape Changing Collisions, and Partially Coherent Solitons in Coupled Nonlinear Schrödinger Equations, Phys. Rev. Lett. 86 (2001), 5043-5046.

[10] T. Kanna, T. E. N. Tsoy and N. Akhmediev, On the solution of multicomponent nonlinear Schrodinger equations, Phys. Lett. A 330 (2004), 224-229.

[11] A. Ankiewicz, W. Krolikowski and N. N. Akhmediev, Partially coherent solitons of variable shape in a slow Kerr-like medium: Exact solutions, Phys. Rev. E 59 (1999), 6079-6087.

[12] N. Akhmediev, W. Krolikowski and A. W. Synder, Partially coherent solitons of variable shape, Phys. Rev. Lett. 81 (1998), 4632-4635.

[13] K. Nakkeeran, Exact dark solition solitions for a family of *N* coupled nonlinear Schrödinger equations in optical fiber media, Phys. Rev. E 64 (2001), 046611.

[14] X. Qian, S. Song and Y. Chen, A semi-explicit multi-symplectic splitting scheme for a 3-coupled nonlinear Schrödinger equation, Computer Physics Communications 185 (2014), 1255-1264.

[15] X. Liang, A. Q. M. Khaliq and Q. Sheng, Exponential time differencing Crank-Nicolson method with a quartic spline approximation for nonlinear Schrödinger equations, Applied Mathematics and Computation 235 (2014), 235-252.

[16] H. P. Bhatt and A. Q. M. Khaliq, Higher order exponential time differencing scheme for system of nonlinear Schrödinger equations, Applied Mathematics and Computation 228 (2014), 271-291.

[17] S. Wang, T. Wang and L. Zhang, Numerical computations for *N*-coupled nonlinear Schrödinger equations by split step spectral methods, Applied Mathematics and Computation 222 (2013), 438-452.

[18] A. Aydin and B. Karasözen, Multi-symplectic integration of coupled non-linear Schrödinger system with soliton solutions, International Journal of Computer Mathematics 86(5) (2009), 864-882.

[19] A. Aydin and B. Karasözen, Symplectic and multisymplectic methods for the coupled nonlinear Schrödinger equations with periodic solutions, Computer Physics Communications 177(7) (2007), 566-583.

[20] N. H. Sweilam and R. F. Al-Bar, Variational iteration method for coupled nonlinear Schrödinger equations, Computers and Mathematics with Applications 54(7-8) (2007), 993-999.

[21] S. C. Tsang and K. W. Chow, The evolution of periodic waves of the coupled nonlinear

Schrödinger equations, Mathematics and Computers in Simulation 66 (2004), 551-564.

[22] M. S. Ismail, Numerical solution of coupled nonlinear Schrödinger equation by Galerkin method, Mathematics and Computers in Simulation 78 (2008), 532-547.

[23] M. S. Ismail, A fourth-order explicit schemes for the coupled nonlinear Schrödinger equation, Applied Mathematics and Computation 196 (2008) 273-284.

[24] T. Wang, B. Gou and L. Zhang, New conservative difference schemes for a coupled nonlinear Schrödinger system, Applied Mathematics and Computation 217 (2010), 1604-1619.

[25] T. Wang, Maximum norm error bound of a linearized difference scheme for a coupled nonlinear Schrödinger equations, Journal of Computational and Applied Mathematics 235(14) (2011), 4237-4250.

[26] Q. Xu and Q. Chang, New numerical methods for the coupled nonlinear Schrödinger equations, Acta Mathematicae Applicatae Sinica, English Series, 26(2) (2010), 205-218.

[27] M. S. Ismail and T. R. Taha, A linearly implicit conservative scheme for the coupled nonlinear Schrödinger equation, Mathematics and Computers in Simulation 74 (2007), 302-311.

[28] R. I. McLachlan, G. R. W. Quispel and N. Robidoux, Geometric integration using discrete gradients, Phil. Trans. Roy. Soc. A 357 (1999), 1021-1046.

[29] G. R. W. Quispel and D. I. McLaren, A new class of energy-preserving numerical integration methods, J. Phys. A 41 (2008), 045206.

[30] D. Cohen and E. Hairer, Linear energy–preserving integrators for Poisson systems, BIT 51 (2011), 91-101.

[31] E. Hairer, Energy-preserving variant of collocation methods, J. Numer. Anal. Ind. Appl. Math. 5 (2010), 73-84.

[32] E. Celledoni, V. Grimm, R. I. Mclachlan, D. I. Mclaren, D. O'Neale, B. Owren and G. R. W. Quispel, Preserving energy resp. dissipation in numerical PDEs using the Average Vector Field method, J. Comutational Physics 231(20) (2012), 6770-6789.

[33] B. Karasözen and G. Simsek, Energy preserving integration of bi-Hamiltonian partial differential equations, Applied Mathematics Letters 26(12) (2013), 1125-1133.

[34] Z. Hon, S. Song-He, C. Xu-Dong and Z. Wei-En, Average vector field methods for the coupled Schrödinger-KdV equations, Chin. Phys. B 23(7) (2014), 070208.

[35] C. Jiang and J. Sun, A high order energy preserving scheme for the strongly coupled nonlinear Schrödinger system, Chin. Phys. B 23(5) (2014), 050202.

[36] Deepmala, A Study on Fixed Point Theorems for Nonlinear Contractions and its Applications, Ph.D. Thesis (2014), Pt. Ravishankar Shukla University, Raipur 492 010, Chhatisgarh, India.

[37] L. N. Mishra, M. Sen and R. N. Mohapatra, On existence theorems for some generalized nonlinear functional-integral equations with applications, Filomat, accepted on March 21, 2016, in press.

[38] V. N. Mishra, Some Problems on Approximations of Functions in Banach Spaces, Ph.D. Thesis (2007), Indian Institute of Technology, Roorkee 247 667, Uttarakhand, India.

[39] V. N. Mishra and L. N. Mishra, Trigonometric Approximation of Signals (Functions) in $L_p(p \geq 1)$ norm, International Journal of Contemporary Mathematical Sciences 7(19) (2012), 909-918.

[40] L. N. Mishra, R. P. Agarwal and M. Sen, Solvability and asymptotic behavior for some nonlinear quadratic integral equation involving Erdélyi-Kober fractional integrals on the unbounded interval, Progress in Fractional Differentiation and Applications 2(3) (2016), 153-168.

[41] Z. Fei, V. M. Perez-Garacia and L. Vazquez, Numerical simulation of nonlinear Schrödinger systems: a new conservative scheme, Appl. Math. Comput. 71 (1995), 164-177.

[42] X. Antonie, W. Bao and C. Besse, Computational methods for the dynamics of the nonlinear Schrödinger/Gross-Pitaevskii equations, Computer Physics Communication 184(12) (2013), 2621-2633.

[43] J. D. Hoffman, Numerical Methods for Engineers and Scientists, McGraw-Hill, 1992.

[44] R. D. Richtmyer and K. W. Morton, Difference Methods for Initial Value Problems, Second Edition, Interscience, 1967.